

Understanding Kondo Peak Splitting and Novel Transport Mechanism in a Single-Electron Transistor

Jongbae Hong and Wonmyung Woo

*Department of Physics and Astronomy & Center for Theoretical Physics,
Seoul National University, Seoul 151-747, Korea*

(Dated: May 26, 2019)

The peculiar behavior of Kondo peak splitting under a magnetic field and bias can be explained by calculating the nonequilibrium retarded Green's function via the nonperturbative dynamical theory (NDT). In the NDT, the application of a lead-dot-lead system reveals that new resonant tunneling levels are activated near the Fermi level and the conventional Kondo peak at the Fermi level diminishes when a bias is applied. Magnetic field causes asymmetry in the spectral density and transforms the new resonant peak into a major peak whose behavior explains all the features of the nonequilibrium Kondo phenomenon. Transport through the new resonant tunneling level is a novel mechanism of current occurring in a single-electron transistor.

Recently, the nonequilibrium Kondo phenomenon has become one of highly debated subjects in condensed matter physics following the observation of the equilibrium Kondo phenomenon in a single-electron transistor (SET) (1). Since this phenomenon simultaneously comprises two theoretically difficult aspects—nonequilibrium and strong correlation, no study can successfully explain these experiments (2, 3). Therefore, a theoretical understanding of this phenomenon would be an essential development in the advancement of condensed matter physics.

Recent fabrication techniques have facilitated the observation of the Kondo phenomenon under the out-of-equilibrium condition. The most attractive aspect of the nonequilibrium Kondo phenomenon is the splitting of the Kondo peak under a magnetic field. This phenomenon has been observed by measuring the differential conductance in an SET (2, 3). According to the experiment performed by Amasha *et al.* (3), interesting experimental results, which have not been successfully explained by theory, can be summarized as follows: (i) splitting vs. magnetic field, which is expressed by a simple relation $\Delta_{K,S} = \Delta_{K,S}^0 + |g|\mu_B B$, where $\Delta_{K,S}$ denotes half of the gap between the split Kondo peaks, the superscript 0 denotes field-independence, and the subscript S denotes particle-hole symmetric case; (ii) splitting vs. gate voltage, which is given by $\Delta_K^0 = \Delta_{K,S}^0 - C_0(V_g - V_{g,0})^2$, where $V_{g,0}$ denotes the gate voltage in the middle of the Coulomb valley and the curvature of the parabola C_0 is field-independent; (iii) splitting vs. Kondo temperature, which appears to be logarithmically decreasing, i.e., $\Delta_K^0(T_K) \propto -C_1 \ln T_K$, where C_1 is also field-independent; and (iv) the maximum Kondo temperature T_{K_m} vs. the critical magnetic field B_C at the splitting threshold, which is nonlinear. One notable issue common to all the abovementioned features is the field-independent behaviors of $\Delta_{K,S}^0$, C_0 , and C_1 . Existing theories (4, 5) cannot explain the field-independent behaviors in (i), (ii), and (iii) and the nonlinear behavior in (iv). These features of Kondo splitting should be simultaneously explained by a single theory. We will discuss these in terms of the results given by the nonperturbative

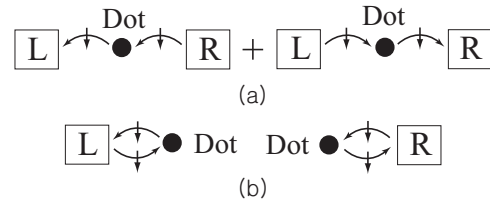


FIG. 1: Motions of spin-down electron in the first (a) and second (b) type of coherence. Z^{LR} and Z^{LL} correspond to (a) and (b), respectively.

dynamical theory (NDT).

It is interesting to observe the creation of two additional resonant tunneling levels when the Anderson model has two separate metallic reservoirs in the form of the left and right leads. The positions of these new resonant levels are independent of the applied magnetic field and bias. The spectral weight of the additional resonant peaks is transferred from the Kondo peak at the Fermi level with an increase in the current. One of these resonant peaks results in a major one in the differential conductance when the magnetic field is applied. All the abovementioned features of the Kondo peak splitting phenomenon can be explained by the position of this major peak. In addition, electron transport through the new resonant tunneling level is very interesting because it is a novel mechanism of electron transport retaining the singlet coupling.

It is natural that only one Kondo peak is located at the Fermi level in the SET during equilibrium (1). The important thing, however, is that this Kondo peak comprises two different types of coherence. We denote the spectral weight of each type as Z^{LR} and Z^{LL} . In the first type of coherence, the spin-down electron, for instance, travels back and forth through the dot as shown in Fig. 1 (a), while it moves as that shown in Fig. 1 (b) in the second type of coherence. The spin-up electron arrives toward the dot from the left or right lead in both the cases.

Under equilibrium, the Fermi level is the only channel

passing through the dot. Therefore, only one coherent peak appears at the Fermi level. Under a bias, however, new resonant tunneling levels are activated by transferring a part of the spectral weight Z^{LL} to the new resonant levels, while the spectral weight Z^{LR} , which corresponds to the first type of coherence, remains at the Fermi level. The effect of the magnetic field and bias results in an asymmetry in the spectral density as well as the usual Zeeman shift for different spins. In addition, the first type of coherence peak located at the Fermi level gets weakened and shifted by the effect of asymmetry. As a result, the newly created resonant peak transforms into a major peak. In Fig. 2, we show a typical form of the spectral density $\rho_{d\uparrow}(\omega)$ of an SET under the nonequilibrium steady state. Because of two separate metallic reservoirs, the maximum of $\pi\Delta\rho_{d\uparrow}(\omega)$ is 0.5 instead of unity. We artificially choose the parameters of the spectral density to show the decoherence of the central peak explicitly. These parameters may be determined by the self-consistent calculation proposed in Ref. (6). Thus, the field-independent part of the splitting behavior shown in (i) is simply expressed by the gap between the major resonant peak and the position of Zeeman splitting $|g|\mu_B B$.

We find that the new resonant peaks are located at $\pm\sqrt{Z_S^{LL}U}/2$ in the Kondo regime with particle-hole symmetry, where U is the amount of Coulomb repulsion at the dot. Therefore, the field-independent splitting in feature (i) mentioned earlier is given by $\Delta_{K,S}^0 = \sqrt{Z_S^{LL}U}/2$. Since asymmetry is involved in the part that becomes U in the symmetric case, we propose the following expression of Δ_K^0 for the asymmetric case:

$$\Delta_K^0 = \sqrt{Z_S^{LL}} \left[\frac{4\sqrt{2}\Gamma}{\pi} \ln \frac{\tilde{D}}{Z\Gamma} \right], \quad (1)$$

where $Z = Z^{LL} + Z^{LR}$ and $\tilde{D} = Z_S\Gamma \exp[\pi U/8\sqrt{2}\Gamma]$. Equation (1) recovers $\Delta_{K,S}^0$ if $Z = Z_S$. If we use the notations given in Ref. (3), the spectral weight Z can be rewritten as $Z = Z_S \exp[\chi(V_g - V_{g,0})^2] = Z_S T_K/T_{K,0}$, where $T_{K,0}$ is the Kondo temperature at $V_g = V_{g,0}$. Then,

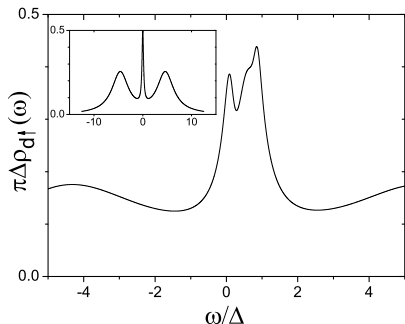


FIG. 2: The spectral density of the SET for $U = 8\Delta$ under a bias, where $\Delta = \Gamma/2$. The Zeeman shift is 0.5Δ . The inset is for that under equilibrium.

the asymmetric behavior of Δ_K^0 is given by the parabolic or logarithmic form

$$\begin{aligned} \Delta_K^0 &= \Delta_{K,S}^0 - \frac{8\sqrt{2}\Gamma}{\pi U} \Delta_{K,S}^0 \chi (V_g - V_{g,0})^2 \\ &= \Delta_{K,S}^0 - \frac{8\sqrt{2}\Gamma}{\pi U} \Delta_{K,S}^0 \ln(T_K/T_{K,0}). \end{aligned}$$

These expressions simultaneously explain all the above-mentioned features of the Kondo peak splitting phenomenon in a qualitative manner, except for the feature of the splitting threshold. The curvature of the parabola and the coefficient in the $-\ln T_K$ -dependence are given by $C_0 = -8\sqrt{2}\Gamma\Delta_{K,S}^0\chi/\pi U$ and $C_1 = 8\sqrt{2}\Gamma\Delta_{K,S}^0/\pi U$, respectively. Since the values of the constants C_0 and C_1 are given by $C_0 = -0.22\mu\text{eV}/(\text{mV})^2$ and $C_1 = 11\mu\text{eV}$, respectively, for $\Gamma = 330\mu\text{eV}$, $U = 1.2\text{meV}$, $\chi = 0.020(\text{mV})^{-2}$, and $\Delta_{K,S}^0 = 11\mu\text{eV}$, quantitative agreement with the experimental data is also perfect.

The threshold of the Kondo peak splitting depends on the positions of the major peaks produced by both the spin-up and spin-down electrons. For a reversed bias, the total spectral density is a mirror-reflected one with respect to the vertical axis. Therefore, when $|g|\mu_B B = \Delta_K^0$, the major peak of $\rho_{d\uparrow}(\omega)$ appears at $2\Delta_K^0$ above the Fermi level, while that of $\rho_{d\downarrow}(\omega)$ is located at the Fermi level. In this case, no separation is observed. The Kondo peak separation may be observed when the major peak of $\rho_{d\downarrow}(\omega)$ appears at a position lower than Δ_K^0 below the Fermi level, i.e., $|g|\mu_B B + \Delta_K^0(T_K) > 3\Delta_K^0(T_{K,0})$. At $T_K = T_{K,0}$, $B_C = 2\Delta_{K,S}^0/|g|\mu_B$, which corresponds to $B_C = 2.4\text{T}$ for $\Delta_{K,S}^0 = 11\mu\text{eV}$ and $|g| = 0.16$ (3). Then, the threshold equation must be written as $|g|\mu_B B_C + \Delta_K^0(T_{K_m}) = 3\Delta_{K,S}^0$, where T_{K_m} is the Kondo temperature at threshold (3), if we do not consider dispersion effect. Since the splitting threshold is considerably influenced by the dispersion due to temperature, we correct the equation as $|g|\mu_B B_C + \Delta_K^0(T_{K_m}) = 3\Delta_{K,S}^0[1 + (T_{K_m} - T_{K,0})/4T_{K,0}]$. It is in remarkable agreement with the experiment as shown in Fig. 3. We used the experimental value $T_{K,0} = 0.25\text{K}$.

We successfully explained the experiments using Eq. (1). Now, we derive Eq. (1) by calculating the retarded on-site Green's function $G_{dd\uparrow}^+(\omega)$ under nonequilibrium conditions. We use the NDT (6) that provides a new

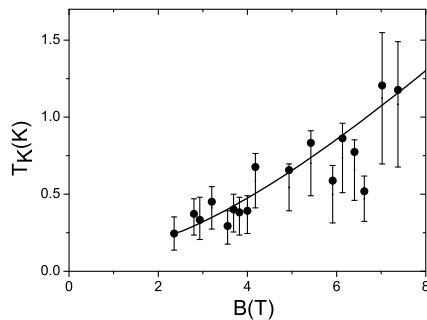


FIG. 3: Relationship between T_{K_m} and B_C at the splitting threshold.

technique to calculate $G_{dd\uparrow}^+(\omega)$, which is expressed as $G_{dd\sigma}^+(\omega) = \langle c_{d\sigma} | (\omega + i\eta - \mathbf{L})^{-1} | c_{d\sigma} \rangle$ in the Heisenberg picture (7), where \mathbf{L} is the Liouville operator defined by $\mathbf{L}A = HA - AH$ where H is the Hamiltonian, η is a positive infinitesimal, and the inner product is defined as $\langle A|B \rangle \equiv \langle \{A^\dagger, B\} \rangle$, where A and B are the operators of the Liouville space, the curly brackets denote the anti-commutator, and the last angular brackets represent a nonequilibrium average (6). If we define the elements of the matrix \mathbf{M} as $\mathbf{M}_{ij} = \langle \hat{e}_i | z\mathbf{I} + i\mathbf{L} | \hat{e}_j \rangle$, where $z = -i\omega + \eta$ and the operator \hat{e}_j is one of the bases spanning the Liouville space, the retarded Green's function is represented by $iG_{dd\sigma}^+(\omega) = \langle c_{d\sigma} | \mathbf{M}^{-1} | c_{d\sigma} \rangle = (\text{adj } \mathbf{M})_{dd} [\det \mathbf{M}]^{-1}$, where $(\text{adj } \mathbf{M})_{ij}$ denotes the cofactor of the ji -element in the determinant of \mathbf{M} .

The NDT is initiated by constructing a complete set of dynamical bases $\{\hat{e}_j | j = 1, 2, \dots, \infty\}$ spanning the reduced Liouville space in which the dynamics of the operator $c_{d\sigma}(t)$ effectively describes the Kondo processes. We simply extend the bases for the single-impurity Anderson model used in the previous study (6) to the case of two metallic reservoirs described by the Hamiltonian $H = \sum_{k,\sigma,\alpha=L,R} \epsilon_k c_{k\sigma}^\alpha c_{k\sigma}^\alpha + \sum_{k,\sigma,\alpha=L,R} (V_{kd} c_{d\sigma}^\alpha c_{k\sigma}^\alpha + V_{kd}^* c_{k\sigma}^\alpha c_{d\sigma}^\alpha) + \sum_{\sigma=\pm 1} (\epsilon_d - \sigma g |\mu_B| B) c_{d\sigma}^\dagger c_{d\sigma} + U n_{d\uparrow} n_{d\downarrow}$, in which L and R denote the left and right leads, respectively, and the subscript k denotes the quantum state of the metallic leads and $n_{d\downarrow} = c_{d\downarrow}^\dagger c_{d\downarrow}$. Then, the basis operators comprise the following five sets: (a) $S_k^L \equiv \{c_{k\uparrow}^L | k = 1, 2, \dots, \infty\}$ for describing the movements in the left noninteracting metallic lead, (b) $S_n^L \equiv \{\delta n_{d\downarrow} c_{k\uparrow}^L | k = 1, 2, \dots, \infty\}$ for describing the annihilation of a spin-up electron in the left lead combined with the density fluctuations in the spin-down electron at the dot, (c) and (d) the sets similar to (a) and (b) for the right lead, i.e., S_k^R and S_n^R , respectively, and (e) $S_d \equiv \{\delta j_{d\downarrow}^{-L} c_{d\uparrow}, \delta j_{d\downarrow}^{+L} c_{d\uparrow}, c_{d\uparrow}, \delta j_{d\downarrow}^{+R} c_{d\uparrow}, j_{d\downarrow}^{-R} c_{d\uparrow}\}$ for describing the dynamical Kondo processes at the dot. Some pictorial descriptions of the basis operators are given in Ref. (6).

If we symmetrically arrange the bases such as $S_k^L, S_n^L, S_d, S_k^R, S_n^R$, and S_k^R to construct the matrix \mathbf{M} , the following matrix of nine blocks is obtained:

$$\mathbf{M}_{\ell d \ell} = \begin{pmatrix} \mathbf{M}_{LL} & \mathbf{M}_{dL} & \mathbf{0} \\ \mathbf{M}_{Ld} & \mathbf{M}_d & \mathbf{M}_{Rd} \\ \mathbf{0} & \mathbf{M}_{dR} & \mathbf{M}_{RR} \end{pmatrix},$$

where the blocks $\mathbf{M}_d, \mathbf{M}_{dL}$ and \mathbf{M}_{dR} , and \mathbf{M}_{Ld} and \mathbf{M}_{Rd} are 5×5 , $5 \times \infty$, and $\infty \times 5$ matrices, respectively. Blocks \mathbf{M}_{LL} and \mathbf{M}_{RR} are the $\infty \times \infty$ matrices that are constructed by the sets of bases describing the left and right leads, respectively. Since no direct coupling exists between the left and right leads, zero matrices occur at the two corners. The structure of each block is similar to that of the corresponding block of the matrix for the Anderson model considered in the previous study (6).

The infinite-dimensional matrix can be reduced to a finite-dimensional matrix using the Löwdin's partition-

ing technique (8, 9). It is performed by solving the eigenvalue equation for the matrix $\mathbf{M}_{\ell d \ell}$, such as $\mathbf{M}_{\ell d \ell} \mathbf{C} = \mathbf{0}$, where \mathbf{C} and $\mathbf{0}$ are the infinite-dimensional column vectors. The column vector \mathbf{C} is partitioned into three parts, i.e., $\mathbf{C}^T = (\mathbf{C}^L \mathbf{C}^d \mathbf{C}^R)$, where T, L, d , and R denote the transpose, left lead, dot, and right lead, respectively. Then, the equation for \mathbf{C}^d is obtained as $(\mathbf{M}_d - \mathbf{M}_{Ld} \mathbf{M}_{LL}^{-1} \mathbf{M}_{dL} - \mathbf{M}_{Rd} \mathbf{M}_{RR}^{-1} \mathbf{M}_{dR}) \mathbf{C}^d \equiv \widetilde{\mathbf{M}}_d \mathbf{C}^d = \mathbf{0}$. The reduced 5×5 matrix $\widetilde{\mathbf{M}}_d$ contains information on the many-body dynamics of the spin-up electron. Obtaining $\widetilde{\mathbf{M}}_d$ is practically possible if the $\infty \times \infty$ matrices \mathbf{M}_{LL} and \mathbf{M}_{RR} are block diagonal (10). The second and third terms appear as self-energies in $\widetilde{\mathbf{M}}_d$ after reduction.

The matrix $\widetilde{\mathbf{M}}_d$ is expressed as

$$\widetilde{\mathbf{M}}_d = \begin{pmatrix} -i\tilde{\omega} & -\gamma_{LL} & -U_{J-}^L & \gamma_{LR} & \gamma_{J-} \\ \gamma_{LL} & -i\tilde{\omega} & -U_{J+}^L & \gamma_{J+} & \gamma_{LR} \\ U_{J-}^{L*} & U_{J+}^{L*} & -i\tilde{\omega} & U_{J+}^{R*} & U_{J-}^{R*} \\ -\gamma_{LR} & \gamma_{J+} & -U_{J+}^R & -i\tilde{\omega} & \gamma_{RR} \\ \gamma_{J-} & -\gamma_{LR} & -U_{J-}^R & -\gamma_{RR} & -i\tilde{\omega} \end{pmatrix}$$

All the matrix elements, other than $U_{J\pm}$ and $U_{J\pm}^*$, have additional self-energy functions $\Sigma_{ij}(\omega) = (1/4 + \beta_{ij})(\Sigma_0^L(\omega) + \Sigma_0^R(\omega))$, where $\Sigma_0(\omega)$ is the self-energy of the noninteracting system. The coefficients β_{ij} vanish when the system exhibits particle-hole symmetry; however, their values are different under a bias and a magnetic field. They are given by $\beta_{11} < \beta_{12} = \beta_{21} < \beta_{22}$ and similar relationships for the other three corners (11). These inequalities cause a reduction in the coherent peak Z_{LR} positioning at the Fermi level. We find that $\gamma_{LL} = \gamma_{RR}$ and $\gamma_{J-} = \gamma_{J+}$.

In particular, it is noteworthy that the matrix equation $\widetilde{\mathbf{M}}_d = \mathbf{0}$ has roots at $\tilde{\omega} = 0$, $\tilde{\omega} = \pm\gamma_{LL}$ and $\tilde{\omega} = \pm U/2$ in the Kondo regime if we consider it in the atomic limit. This implies that there are additional resonant tunneling levels at $\pm\gamma_{LL}$ if we treat the system with two separate leads. One of the effects of the magnetic field is the Zeeman shift $\omega' - g|\mu_B|B \equiv \tilde{\omega}$, where $\omega' = \omega - \epsilon_d - U\langle n_{d\downarrow} \rangle$, appearing in the diagonal elements. We use ω to represent ω' hereafter. The Zeeman shift results in a nonvanishing value of $1/2 - \langle n_{d\downarrow} \rangle$ that induces asymmetry in the spectral density by the nonvanishing imaginary part of the elements $U_{J\pm}$, which can be expressed as $U_{J\pm} = (U/4) + i(1 - 2\langle n_{d\downarrow} \rangle) \langle j_{d\downarrow}^\pm \rangle$. The asymmetry maximizes the new resonant peak appearing at $\omega = g\mu_B B + \gamma_{LL}$, as shown in Fig. 2. Therefore, the field-independent splitting Δ_K^0 is merely γ_{LL} . The real part of $U_{J\pm}$ determines the positions of the U peaks. The coefficient $1/4$ was determined from the analysis performed at the atomic limit. It is $1/\sqrt{2}$ times smaller than that of the single impurity Anderson model (6).

Since $\gamma_{LL} = \langle \sum_k i(V_{kd}^{*L} c_{k\uparrow}^L + V_{kd}^{*R} c_{k\uparrow}^R) c_{d\uparrow}^\dagger [j_{d\downarrow}^{-L}, j_{d\downarrow}^{+L}] \rangle$, its direct calculation is difficult. Therefore, we employ

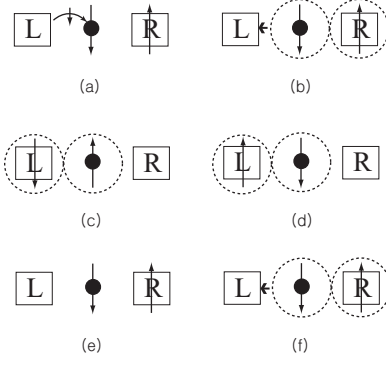


FIG. 4: Transport mechanism of the spin-up electron through the new resonant tunneling level.

an indirect way to obtain the calculable expression for γ_{LL} . One can easily find the spectral weight at $\omega = 0$, which represents the wavefunction renormalization Z . Under equilibrium with particle-hole symmetry, it is expressed as $Z_S = [1 + U^2/\{4(\gamma_{LL}^2 + \gamma_{LR}^2)\}]^{-1}$, where $\gamma_{LR} = \langle \sum_k i(V_{kd}^* c_{k\uparrow}^L + V_{kd}^* c_{k\uparrow}^R) c_{d\uparrow}^\dagger [j_{d\downarrow}^{-L}, j_{d\downarrow}^{+R}] \rangle$. In the Kondo regime, Z_S gets separated into two parts, i.e., $Z_S^{LL} = 4\gamma_{LL}^2/U^2$ and $Z_S^{LR} = 4\gamma_{LR}^2/U^2$. The latter is the spectral weight remaining at the Fermi level, which does not contribute to the Kondo peak splitting, and the former gives rise to the additional shift $\Delta_{K,S}^0 = \gamma_{LL} = \sqrt{Z_S^{LL}}U/2$ to the one by Zeeman effect.

Since γ_{LL} is independent of the Coulomb repulsion, U may be expressed by the wavefunction renormalization. The theory using Bethe ansatz yields $Z_S = (4/\pi)\sqrt{U/\Gamma}\exp[-\pi U/4\Gamma]$ for the symmetric Anderson model in the Kondo regime (12). Then, U is written as $U = (4\Gamma/\pi)\ln(\tilde{D}/Z_S\Gamma)$, where $\tilde{D} = Z_S\Gamma\exp[\pi U/4\Gamma]$. For the Anderson model with two separate reservoirs, however, the effect of the two reservoirs changes U and Γ into $U/\sqrt{2}$ and 2Γ , respectively. Therefore, $Z_S = (4/\pi)\sqrt{U/2\sqrt{2}\Gamma}\exp[-\pi U/8\sqrt{2}\Gamma]$ for the SET in the Kondo regime. By using the expression for U and changing Z_S into Z to take the asymmetry into account, we write $\gamma_{LL} = (4\sqrt{2}\Gamma/\pi)\sqrt{Z_S^{LL}}\ln(\tilde{D}/Z\Gamma)$, where $\tilde{D} = Z_S\Gamma\exp[\pi U/8\sqrt{2}\Gamma]$. This is just Eq. (1).

It is interesting and meaningful to observe the mechanism of electron transport through the new resonant tunneling level in an SET. This mechanism appears in the operator expressions of γ_{LL} . The motion of the spin-down electron is governed by the operator $[j_{d\downarrow}^{-L}, j_{d\downarrow}^{+L}]$, as described in Fig. 1 (b), while the spin-up electron moves into the dot from the left or the right lead. Since the movement that costs energy U is not allowed, a possible operation that constitutes a current is the one in which a spin-down electron moves from the left lead to

the dot, makes a singlet coupling with a spin-up electron on the right lead, and reverts together toward the left lead. Then, after a virtual exchange, the process is repeated. Figure 4 shows this process. This is a novel and unique way of a current flowing through the new resonant tunneling level in an SET with a strong correlation. It is noteworthy that the singlet state is retained during transport, similar to that in superconductivity.

The motion of the spin-down electron of the operator $[j_{d\downarrow}^{-L}, j_{d\downarrow}^{+R}]$ in γ_{LR} is shown in Fig. 1 (a), while that of the operator $[j_{d\downarrow}^{\mp L}, j_{d\downarrow}^{\mp R}]$ in $\gamma_{J\mp} = \langle \sum_k i(V_{kd}^* c_{k\uparrow}^L + V_{kd}^* c_{k\uparrow}^R) c_{d\uparrow}^\dagger [j_{d\downarrow}^{\mp L}, j_{d\downarrow}^{\mp R}] \rangle$ is equal to Fig. 1 (a) if we change the + sign with -, which corresponds to the net flow of the spin-down electrons. When the bias increases, $\gamma_{J\mp}$ approaches γ_{LR} and the spectral weight of the new resonant peak also increases. However, at equilibrium, $\gamma_{J\mp}$ vanishes and the new resonant peak disappears.

In conclusion, we report the existence of a new resonant tunneling level in an SET with a strong correlation. This new resonant tunneling level is activated only under nonequilibrium conditions, and it explains all the features of the Kondo peak splitting phenomenon measured by Amasha *et al.* (3). Further, we report a novel transport mechanism through the new resonant tunneling level.

References and notes

- (1) D. Goldhaber-Gordon *et al.*, Nature (London) **391**, 156 (1998); D. Goldhaber-Gordon *et al.*, Phys. Rev. Lett. **81**, 5225 (1998).
- (2) A. Kogan *et al.*, Phys. Rev. Lett. **93**, 166602 (2004).
- (3) S. Amasha *et al.*, Phys. Rev. B **72**, 045308 (2005).
- (4) J. E. Moore, X.-G. Wen, Phys. Rev. Lett. **85**, 1722 (2000).
- (5) T. A. Costi, Phys. Rev. Lett. **85**, 1504 (2000).
- (6) J. Hong, W. Woo, preprint available at <http://xxx.lanl.gov/abs/cond-mat/0701765>.
- (7) P. Fulde, *Electronic Correlations in Molecules and Solids* (Springer-Verlag, Berlin, 1993).
- (8) P. O. Löwdin, J. Math. Phys. **3**, 969 (1962).
- (9) V. Mujica, M. Kemp, M. A. Ratner, J. Chem. Phys. **101**, 6849 (1994).
- (10) A. S. Householder, *Principles of Numerical Analysis* (McGraw-Hill, New York, 1953), pp. 78.
- (11) The expressions for β_{ij} are given by $\beta_{ij} = 4(\Delta n_{d\downarrow})^2/\sigma_{ij}^2(j_{d\downarrow}^\pm)$, where $j_{d\downarrow}^\mp = i(\sum_k V_{kd} c_{k\downarrow}^\dagger c_{d\downarrow} \mp \sum_k V_{kd}^* c_{d\downarrow}^\dagger c_{k\downarrow})$, $(\Delta n_d)^2 = (1/2 - \langle n_d \rangle)^2$, and $\sigma^2(j^\pm) = \langle (\delta j^\pm)^2 \rangle / \langle j^\pm \rangle^2$. σ_{11} and σ_{22} correspond to j^- and j^+ , respectively, while $\sigma_{12} = \sqrt{\langle (\delta j^-)^2 \rangle \langle (\delta j^+)^2 \rangle} / \langle j^- \rangle \langle j^+ \rangle$.
- (12) A. C. Hewson, *The Kondo Problem to Heavy Fermions* (Cambridge University Press, Cambridge, UK, 1993).
- (13) This work was supported by the Korea Research Foundation, Grant No. KRF-2006-0409-0060.